

Optimal Timing of Organs-at-Risk-Sparing Adaptive Radiation Therapy for Head-and-Neck Cancer under Re-planning Resource Constraints

Fatemeh Nosrat^{1,†}, Cem Dede^{2,‡}, Lucas B. McCullum^{2,3,‡}, Raul Garcia^{1,†}, Abdallah S. R. Mohamed^{2,4,‡}, Jacob G. Scott⁵, James E. Bates⁶, Brigid A. McDonald^{2,‡}, Kareem A. Wahid^{2,‡}, Mohamed A. Naser^{2,‡}, Renjie He^{2,‡}, Aysenur Karagoz^{1,†}, Amy C. Moreno^{2,‡}, Lisanne V. van Dijk^{2,7}, Kristy K. Brock⁸, Jolien Heukelom⁹, Seyedmohammadhossein Hosseinian^{10,†}, Mehdi Hemmati^{11,†}, Andrew J. Schaefer^{1,†}, Clifton D. Fuller^{1,2,†,‡}¹

¹Department of Computational Applied Mathematics and Operations Research, Rice University, Houston, TX, USA

²Department of Radiation Oncology, The University of Texas MD Anderson Cancer Center, Houston, TX, USA

³The University of Texas MD Anderson Cancer Center UTHealth Houston Graduate School of Biomedical Sciences, Houston, TX, USA

⁴Department of Radiation Oncology, Baylor College of Medicine, Houston, TX, USA

⁵Department of Translational Hematology and Oncology Research, Lerner Research Institute, Cleveland, OH, USA

⁶Department of Radiation Oncology, Emory University, Atlanta, GA, USA

⁷Department of Radiation Oncology, University of Groningen, University Medical Center Groningen, Groningen, Netherlands

⁸Department of Imaging Physics, The University of Texas MD Anderson Cancer Center, Houston, TX, USA

⁹Department of Radiation Oncology (Maastrro), GROW School for Oncology and Reproduction, Maastricht University Medical Centre+, Maastricht, Netherlands

¹⁰Edward P. Fitts Department of Industrial and Systems Engineering, North Carolina State University, Raleigh, NC, USA

¹¹School of Industrial and Systems Engineering, University of Oklahoma, Norman, OK, USA

Corresponding Authors: Fatemeh Nosrat (fatemeh.nosrat@rice.edu); Andrew J. Schaefer (andrew.schaefer@rice.edu); Clifton D. Fuller (cdfuller@mdanderson.org)

Abstract word count: 244

Manuscript word count: 3531

[†]On behalf of the Rice/MD Anderson Center for Operations Research in Cancer (CORC)

[‡]On behalf of the MD Anderson Head and Neck Cancer Symptom Working Group

1 **Abstract.**

2 *Background and Purpose:* Prior work on adaptive organ-at-risk (OAR)-sparing radiation
3 therapy has typically reported outcomes based on fixed-number or fixed-interval re-planning,
4 which represent one-size-fits-all approaches and do not account for the variable progression
5 of individual patients' toxicities. The purpose of this study was to determine the
6 personalized optimal timing for re-planning in adaptive OAR-sparing radiation therapy,
7 considering limited re-planning resources, for patients with head and neck cancer (HNC).

8 *Materials and Methods:* A novel Markov decision process (MDP) model was developed
9 to determine optimal timing of re-planning based on the patient's expected toxicity,
10 characterized by normal tissue complication probability (NTCP), for four toxicities. The
11 MDP parameters were derived from a dataset comprising 52 HNC patients treated at the
12 University of Texas MD Anderson Cancer Center between 2007 and 2013. Kernel density
13 estimation was used to smooth the sample distributions. Optimal re-planning strategies were
14 obtained when the permissible number of re-plans throughout the treatment was limited
15 to 1, 2, and 3, respectively.

16 *Results:* The MDP (optimal) solution recommended re-planning when the difference between
17 planned and actual NTCPs (Δ NTCP) was greater than or equal to 1%, 2%, 2%, and 4%
18 at treatment fractions 10, 15, 20, and 25, respectively, exhibiting a temporally increasing
19 pattern. The Δ NTCP thresholds remained constant across the number of re-planning
20 allowances (1, 2, and 3).

21 *Conclusion:* In limited-resource settings that impeded high-frequency adaptations, Δ NTCP
22 thresholds obtained from an MDP model could derive optimal timing of re-planning to minimize
23 the likelihood of treatment toxicities.

24
25 *Keywords:* Personalized adaptive radiation therapy, organs at risk, normal tissue complication
26 probability, Markov decision process, optimal strategy

27 **1 Introduction**

28 Advancements in radiation delivery techniques, such as intensity-modulated radiation therapy
29 (IMRT) and volumetric-modulated arc therapy, enable accurate dose delivery to tumor targets
30 while minimizing radiation exposure of the surrounding organs at risk (OARs) [1]. However,
31 anatomical changes during the treatment, such as weight loss or tumor shrinkage, may cause the
32 actual delivered dose to OARs to deviate from the planned dose. This can increase the risk of
33 treatment-induced toxicities, particularly in cases where multiple OARs are in close proximity to the
34 target, as in head and neck cancer (HNC) [2–4]. To address this, adaptive radiation therapy (ART)
35 has been clinically introduced, proposing on-therapy re-planning in response to anatomical changes
36 in the target and OARs [5–10].

37 In practice, however, the clinical implementation of ART with daily (or even less-frequent) re-
38 planning remains limited, in large part due to the extensive human/personnel/workflow resources
39 required to frequently perform key tasks such as segmentation and quality assurance as well as
40 limited device accessibility time [11, 12]. Recent artificial intelligence (AI)-based algorithms (such

41 as auto-segmentation or synthetically created CTs) [13, 14] may mitigate some or all of these process
42 level frictions; however, the integration of such AI tools within the ART workflow is still evolving
43 [15]. With the advent of hybrid MR-Linac devices, real-time adjustment of daily radiation plans,
44 known as on-line ART, is now a possibility. On-line ART can also be enabled with the availability
45 of high-frequency, high-quality cone- beam CT or CT-on-Rails devices [16, 17]. Regardless of ART
46 implementation imaging inputs (MR or CT), cancer centers in the U.S. typically have implemented
47 ART at fixed intervals, notably once mid-therapy [18] and often as a ‘verification’ of re-simulation.
48 Most of the relevant studies also only report outcomes on fixed-number and/or fixed-interval re-
49 planning [19–21] (see Supplementary Table A1 for a comprehensive literature review). Such pre-
50 determined schedules for treatment re-planning, however, take a one-size-fits-all approach and do not
51 account for the uncertain trajectory of individual patients’ toxicities [21], nor patient-specific tumor
52 regression. As a result, determining the optimal timing of re-planning episodes remains a crucial
53 unmet need, particularly for OAR-sparing adaptive approaches (whether for MR-Linac as we have
54 implemented in MR-guided clinical trials [19] or for analogous CT-based approaches [20]).

55 Heukelom et al. [22] investigated the optimal implementation of ART with a single re-planning
56 allowance (in OAR-sparing radiation therapy) using daily on-treatment CT imaging with a CT-on-rails
57 device. Leveraging the same dataset, this paper presents a new analytical approach to derive optimal
58 re-planning strategies based on Markov decision process (MDP) models. Our aim is to identify the
59 optimal timing for re-planning based on changes in normal tissue complication probabilities (NTCP)
60 of four toxicities: xerostomia, dysphagia, parotid gland dysfunction, and feeding tube dependency at 6
61 months post-treatment. We further include allowances in HNC treatment plan adaptations (through
62 limiting the number of available re-plans) to enhance personalized treatment and efficacy. MDPs
63 constitute a class of mathematical optimization models that aim to determine optimal decisions/actions
64 in stochastic dynamic systems [23, 24]. MDPs have been successfully employed to find the optimal
65 timing for various medical interventions [25–31]; however, to our knowledge, MDPs have not been
66 applied for triggering adaptive re-planning. We develop a generalized framework for the utilization
67 of MDPs for evidence-based individualized radiation treatment re-planning, scalable across resource-
68 rich and resource-limited facilities, and applicable to both CT- and MR-based platforms. Thus,
69 rather than a class solution based on population estimates of toxicity reduction potential, we enable
70 personalized adaptive therapy with consideration of a budget.

71 **2 Materials and Methods**

72 *2.1 Data*

73 This study used a prior dataset of CT-on-Rails image-guided radiation therapy (IGRT), detailed
74 by Heukelom et al. [22], which comprised information from patients treated for HNC at the
75 University of Texas MD Anderson Cancer Center between 2007 and 2013; this retrospective
76 secondary analysis was performed under MD Anderson Cancer Center Institutional Review Board
77 approval (MDA RCR03-0800). The treatments involved (chemo-) radiotherapy with daily CT-on-
78 Rails IGRT. Of the 52 patients, 36 were male and 16 were female. Among them, 46 patients
79 were aged 18-65, while the remaining 6 were older than 65. The primary cancer sites were as

80 follows: Larynx (1 patient), Oropharynx (13), Oral cavity (4), Hypopharynx (0), Nasopharynx (15),
 81 and Sinonasal (12). Treatment modalities included radiotherapy alone (16 patients), induction
 82 chemotherapy followed by radiotherapy (2), induction chemotherapy followed by concurrent
 83 chemoradiation (16), concurrent chemoradiation (14), and radiation plus Cetuximab (4). The
 84 patients' characteristics are summarized in Supplementary Table B1.

85 **Table 1.**

86 Observed Δ NTCP values based on the difference between planned dose and actual dose,
 87 along with the number of patients associated with each Δ NTCP value. Adapted from
 88 [22] with permission.

89 (a) Fraction 10

Δ NTCP	0%	1%	2%	3%	4%	5%	6%	7%	8%	9%	10%	11%	12%
Number of Patients	26	7	4	6	2	2	0	1	0	0	1	1	2

90 (b) Fraction 15

Δ NTCP	0%	1%	2%	3%	4%	5%	6%	7%	8%	9%	10%	11%	12%
Number of Patients	23	8	9	2	2	1	1	2	0	0	2	1	1

91
 92
 93 For these 52 HNC patients, Heukelom et al. [22] calculated deviation of the actual dose from the
 94 planned dose for nine OARs at fractions 10 and 15 of the treatment. At each fraction, they estimated
 95 NTCP for the toxicities related to the OARs (xerostomia, dysphagia, parotid gland dysfunction, and
 96 tube feeding dependency at 6 months post-treatment) by projecting the actual dose through the
 97 remainder of the treatment period. Subsequently, they compared these findings with the planned
 98 NTCPs and determined the difference, i.e., Δ NTCP, for each toxicity. The NTCP models are
 99 presented in Supplementary Table E1. The MDP model presented in this paper used the Δ NTCP
 100 from this dataset [22], which are summarized in Table 1. For each observed Δ NTCP value,
 101 Heukelom et al. [22] reported the number of patients for whom this Δ NTCP was the highest value
 102 among the four NTCP models.

103
 104 **2.2 Decision Model**

105 In the MDP model, estimates of an individual patient's toxicity outcome, as a function of the
 106 delivered radiation dose to OARs, determine the state of the system at each decision epoch during
 107 the treatment (e.g., day). Depending on the observed state, the clinician may decide between two
 108 possible actions: (1) Re-plan or (2) continue with the current plan. When the action is to continue
 109 with the current plan, the system may transition from one toxicity state to another stochastically,
 110 governed by transition probabilities. Re-planning changes the probabilistic transition towards more
 111 favorable outcomes/states. Given that a limited number of 're-planning' actions may be taken

112 throughout the treatment, an optimal solution to the MDP identifies the optimal timing for taking
113 such actions, as a function of the toxicity states. The MDP model captures the stochastic evolution
114 of post-treatment toxicity risk and identifies optimal re-planning times to mitigate the toxicities
115 (if necessary). The model components are as follows:

116 **Re-planning allowance:** Depending on available resources for plan adaptations, the model
117 considered a maximum number of re-plans B that could be implemented throughout the treatment. The
118 analysis was performed for $B = 1, 2, 3$.

119 **Decision epochs:** Given a treatment period consisting of 33-35 fractions, the decision epochs were
120 set at fractions 10, 15, 20, and 25. Prior studies have shown that anatomical changes are unlikely
121 to happen very early during the treatment [22]; thus fraction 5 was omitted. Fraction 30 was also
122 excluded due to its proximity to the end of treatment, with negligible impact on the total dose to
123 the OARs.

124 **States:** At each decision epoch, the state of the system was captured by the pair $(\Delta\text{NTCP}, b)$,
125 where ΔNTCP denoted the deviation of treatment toxicity from the planned value at that time, and
126 $b \leq B$ was the number of remaining re-plans. For example, if the maximum permissible number
127 of re-plans was 2 ($B = 2$), and the clinician opted to implement a re-plan at fraction 10, then the
128 state of the system at fraction 15 became $b = 1$. The ΔNTCP ranged from 0% to 12% in the model
129 (Table 1); in computing the number of cases for each reported ΔNTCP value, only those patients
130 were included who experienced the change of ΔNTCP in at least one of the four aforementioned
131 toxicities.

132 **Actions:** At each decision epoch, two possible actions were included: (1) Re-planning, or (2)
133 continuing with the current plan (no re-planning). The stochastic transition of the toxicity state
134 from one decision epoch to the next was a function of the action taken and was determined by the
135 associated transition probabilities. Fig. 1 illustrates the states of the MDP and possible transitions
136 associated with each action at Fractions 10, 15, and 20 along with their smoothed transition
137 probabilities, for the case that at most 2 re-plannings may be performed.

138 **Transition Probabilities:** The transition probabilities, governing the stochastic evolution of toxicity
139 under each action, were estimated using the information presented in Table 1. Under the ‘no re-
140 planning’ action, the probabilities for transitions from fraction 0 to 10 and from fraction 10 to 15
141 were directly estimated based on the number of patients in each ΔNTCP category. For example, the
142 probability of transitioning from $\Delta\text{NTCP} = 0\%$ at fraction 0 to $\Delta\text{NTCP} = 1\%$ at fraction 10 is $7/52$
143 $= 0.13$, as 7 patients out of 52 exhibited such a change in ΔNTCP from fraction 0 to fraction 10. To
144 make our transition probabilities more realistic with a broader spread and to avoid any deterministic
145 transitions between states, we smoothed out the transition probability matrix from Fraction 10 to
146 15 by using kernel density estimation with Gaussian kernels, implemented in Python [27]. We
147 manually varied the bandwidth between 0 and 1 to observe its effect on the distribution. Based on
148 these tests, we selected a final bandwidth of 0.4, balancing smoothness and fit to capture
149 meaningful data patterns without introducing noise. The original and smoothed probabilities
150 associated with the ‘no re-planning’ action are presented in Supplementary Material C. It was

151 assumed that transition probabilities from fraction 10 to 15 remained constant for subsequent
152 decision epochs, due to the absence of reported Δ NTCP information beyond fraction 15 by Heukelom
153 et al. [22]. To model the impact of the ‘re-planning’ action on transition probabilities, it was assumed
154 that, at each decision epoch, the action immediately decreased Δ NTCP to a value proportional to the
155 elapsed treatment time. For example, if the ‘re-planning’ action was taken at fraction 10 for
156 Δ NTCP = 5%, the state of toxicity would immediately decreased to Δ NTCP = 2% at this fraction,
157 as approximately one third of the treatment period had passed and the dose escalation would not
158 continue through the rest of the treatment; see Fig. 2. Subsequently, the transition from fraction 10 to
159 15 was governed by the probabilities for Δ NTCP = 2%, calculated from Table 1. The probabilities
160 associated with the ‘re-planning’ action, as described above, are presented in Supplementary Material
161 C.

162 **Rewards:** For each set of consecutive actions taken at the decision epoch, the model considered
163 the expected $-\Delta$ NTCP at the end of the treatment period (with respect to the transition
164 probabilities) as the corresponding reward. The objective of the MDP was to maximize the
165 expected reward by identifying an optimal set of actions, one at each decision epoch, as a function
166 of the system’s state. This is referred to as an optimal policy. Because the rewards were defined
167 by negative values in the MDP model, smaller end-treatment Δ NTCP values translated to higher
168 rewards.

169 The optimal policy of an MDP may become a single-threshold policy (also referred to as
170 control-limit policies) [24], which refers to a class of policies that use thresholds on the state value
171 to recommend an action. For this study, a single-threshold policy recommended re-planning when
172 the Δ NTCP exceeded a threshold, while no re-planning was needed when it falls below the
173 threshold. This implies that if the action for Δ NTCP = $x\%$ at a certain decision epoch was to re-
174 plan, then for every other state with Δ NTCP = $y\% > x\%$ and the same allowance b , the action was
175 also to re-plan. A single-threshold policy reduces the complexity of decision-making to a simple
176 rule that uses only one threshold at each fraction to trigger action and is efficient to implement.

177 The MDP was solved using the MDPtoolbox of MATLAB [32], for $B = 1, 2, 3$. The
178 MATLAB code and its outputs are available at <https://figshare.com/s/64bc3481737d17fc287e>.

179

180 **3 Results**

181 After solving the MDP, the optimal policy, which specified the optimal action (‘re-planning’ or ‘no
182 re-planning’) for each state (Δ NTCP, b) at each decision epoch, was reported. The analysis revealed
183 that the optimal policy was a single-threshold policy, where a specific Δ NTCP threshold was assigned
184 to each fraction. When only one re-plan was allowed ($B = 1$), the optimal policy at fraction 10 was
185 to re-plan for any Δ NTCP value greater than or equal to 1%. Subsequently, at fraction 15, this
186 threshold increased to 2% and remained at 2% for fraction 20. At fraction 25, the minimum Δ NTCP
187 required for a re-planning was 4%. These thresholds remained the same in the optimal policies for B
188 = 2, 3. We summarized the results in Table 2 and provided an illustration in Supplementary Fig.

189 D1 for $B = 3$.

190 **Table 2.**

191 Optimal re-planning thresholds based on Δ NTCP and re-planning allowance.

Re-planning allowance (B)	1		2		3	
Number of remaining re-plans (b)	1	2	1	2	3	1
Δ NTCP threshold at fraction 10	1%	1%	-	-	1%	-
Δ NTCP threshold at fraction 15	2%	2%	2%	-	2%	-
Δ NTCP threshold at fraction 20	2%	2%	2%	-	2%	2%
Δ NTCP threshold at fraction 25	4%	4%	4%	-	4%	4%

192

193 **4 Discussion**

194 This study introduced the first — to our knowledge — application of the mathematically rigorous
195 MDP methodology, to determine optimal timing of ART in HNC. The MDP model guides
196 clinicians in determining the minimum values of Δ NTCP at fractions 10, 15, 20, and 25 for
197 performing a re-plan, given a re-planning allowance of 1, 2, or 3 throughout the treatment.

198 The re-planning Δ NTCP threshold increased over time in the optimal policy, consistent with the
199 diminishing impact of re-planning as the treatment progresses. These values were 1% at fraction
200 10, 2% at fractions 15 and 20, and 4% at fraction 25. Additionally, the results suggest optimality of
201 re-planning for any changes in NTCP (Δ NTCP ≥ 1) at fraction 10. This supports the findings of
202 Heukelom et al. [22], who identified fraction 10 as the optimal time for a single re-plan. Importantly,
203 at a given fraction, the Δ NTCP thresholds remained the same for different number of re-plans ($B = 1,$
204 $2, 3$); the re-planning allowance did not affect these thresholds. Furthermore, in cases where Δ NTCP
205 at fraction 25 was below the 4% threshold, both options (‘re-planning’ or ‘no re-planning’) yielded
206 the same impact on the end-treatment Δ NTCP, indicating that re-planning did not result in an
207 improvement.

208 We acknowledge that minimizing the expected Δ NTCP may result in prescribing re-planning
209 for any Δ NTCP value, potentially leading to a high number of false negatives. This arises from
210 our modeling assumptions, which permitted a fixed number of re-plans at no cost, encouraging
211 frequent re-planning due to low Δ NTCP thresholds. In an ongoing study, we are incorporating re-
212 planning costs without limiting the number of re-plans to better explore the trade-off between cost
213 and benefit; however, at a minimum, we have opted to err on the side of patient benefit, rather than cost-
214 control; as patient NTCP benefit is potentially scalable across any health system, while cost per re-plan
215 and acceptable cost constraints are variable across national and international health policy and
216 reimbursement systems.

217 The significance of a Δ NTCP of 4% or below lies in its potential impact on patient outcomes.
218 While seemingly minor, even slight decreases in NTCP can have considerable implications for
219 patient health and well-being. For instance, a reduction in severe toxicity such as osteoradionecrosis
220 by just 4% could significantly enhance the quality of life and long-term survival prospects for
221 patients. Moreover, customizing treatment to achieve such reductions underscores the importance of

222 personalized care tailored to individual patient needs. By focusing on optimizing treatment outcomes
223 at this level, healthcare practitioners can prioritize patient-centric approaches that aim to minimize
224 treatment-related toxicity and maximize overall patient benefit.

225
226 We leveraged an existing CT-on-rails reference dataset [22] to objectively derive the Δ NTCP
227 listed in the proposed MDP model. It is crucial to acknowledge the limitations regarding the
228 generalizability of findings from this single-site retrospective in silico dataset. For instance, the in
229 silico daily dose accumulation was not actively applied to individual patients, but rather calculated
230 post hoc from a high-granularity CT-on-rails daily volumetric IGRT series. The CT-on-rails platform
231 at MD Anderson utilized an in-house custom-constructed intermediary localization and
232 alienation software (CT-Assisted Targeting (CAT)) [33]. Consequently, there were instances where
233 delivered geometric shifts were either unrecorded or unrecoverable, or clearly aberrant (such as extensive
234 shift records representing an initial setup that was then revised after repositioning) during the
235 secondary export of coordinate displacement to the commercial Record and Verify software
236 (Mosaiq, Elekta AB). These discrepancies were subsequently omitted in the in-silico model to
237 streamline data, leading to conceptual gaps in the resultant NTCP modeling where these missing
238 values were not accounted for. Furthermore, it is important to note that this modeled secondary
239 dataset did not include adaptation or daily re-optimization of the initial daily dose in vivo.
240 Consequently, the data presented in this paper should be viewed as a clinically approximate semi-
241 synthetic illustrative use-case, rather than a definitive rationale for the large-scale implementation of
242 the observed idealized re-planning thresholds across distinct operational platforms. Nonetheless, we
243 believe that the resultant MDP model could be readily scaled using higher-quality prospective or
244 observational cohort data for secondary validation. In essence, the data presented in this paper
245 should be regarded as informative rather than definitive, and the individualized planning parameters
246 suggested by MDP should be viewed as proof of concept rather than a formal criterion barring
247 external validation.

248 In the prior work, Heukelom et al. [22] exclusively reported Δ NTCP for fractions 10 and 15,
249 consistent with internal re-planning practices at MD Anderson Cancer Center based on data from a
250 Phase II study by Maki et al. [34]. Consequently, for model extensibility in the current application,
251 we have explicitly assumed transition probabilities remain stable for the subsequent epochs. This
252 assumption introduced a known level of uncertainty that warrants consideration and is an area of
253 future research, as it has been unclear for specific OARs whether these transition states were indeed
254 stable over therapy. Moreover, the MDP model stipulated weekly re-planning intervals on indexed
255 fractions (e.g., fractions 10, 15, 20, 25, and 30) as a simplification for clarity of presentation reflective
256 of our current adaptive protocols [19], but could readily be adapted to continuous daily fraction-based
257 re-planning intervals.

258 The four NTCP models in Supplementary Table E1 are among the most currently used models
259 to calculate the NTCP values for the considered toxicities: xerostomia, dysphagia, parotid gland
260 dysfunction, and feeding tube dependency at 6 months post-treatment [22, 35]. With the advent of
261 more recent NTCP models for HNC radiation therapy, e.g., [36], it is possible that new NTCP models

262 could offer improved estimations. In addition, the presented results are based on data collected from
263 52 HNC patients. While we recognize the importance of sample size in calibrating MDPs, this
264 sample size is considered substantial in HNC research, considering that HNC accounts for only
265 about 4% of cancer cases in the United States [37]. Furthermore, our results are contingent upon
266 the available CT-on-Rails data, and future research may benefit from incorporating higher-
267 dimensional data (e.g., GTV/the clinical target volume (CTV) modifying approaches, MRI anatomic
268 and/or biomarker data for TCP/NTCP) for a more extensive insight.

269 Nonetheless, the proposed MDP model for ART is clinically relevant, mathematically rigorous,
270 resource-aware, and scalable, and can be adjusted based on new OAR toxicity with reference
271 NTCP values. Necessarily, the precision of the model relies on accurate calculations of NTCP,
272 particularly when adhering to rigorous criteria that determine whether patients are suitable for or
273 excluded from ART [38]. Despite the challenges and limitations, our study introduces novel
274 contributions to the field of ART. Unlike previous works [22], which primarily considered a single
275 re-planning allowance, our optimization model extends its applicability to scenarios with multiple
276 re-plans. Furthermore, our optimal policy spans across fractions 10, 15, 20, and 25, representing
277 an advancement beyond the limited scope of Heukelom et al. [22], which only reported results for
278 fractions 10 and 15. Gan et al. [39] achieved optimal timing for re-planning in HNC radiation
279 therapy by analyzing weekly dose data through semi-auto segmentation and the K-nearest-
280 neighbor method. They constructed a dose deviation map to visualize differences between planned
281 and actual doses, simulating different ART scenarios. By evaluating accumulated dose differences
282 before and after re-planning, the optimal timing for re-planning was determined. Our methodology
283 differs in that we incorporate Δ NTCP and utilize it to develop an MDP model for determining the
284 optimal timing for re-planning.

285 An aspect not explored in this study is the adaptation based on GTV or CTV modification, either
286 for shrinking GTV/CTVs [19] or isotoxic boost approaches [40, 41]; we concentrated solely on
287 OAR-based adaptation. Adapting based on GTV could open avenues for optimal re-plans,
288 potentially influencing NTCP and extending into scenarios such as Stereotactic Body RT [42]. This
289 introduces a distinctive problem and solution space beyond the scope of our current investigation.
290 Furthermore, we exclusively focused on optimizing the ART workflow within the context of photon
291 therapy. Similar optimization methodologies could prove advantageous when exploring ART in the
292 context of proton therapy, particularly in addressing setup variability reduction [43]. For this study,
293 NTCP calculations were based on the ‘plan of the day.’ While our findings may vary with deformable
294 dose registration, the operational implementation remains consistent. Future efforts should consider
295 incorporating deformable dose registration to enhance the model’s generalization.

296 Several surveys in both low/middle-income countries [44, 45] and high-income economies [45]
297 have identified resource constraints as an impediment to ART implementation; the use of models
298 such as our MDP provides a potential avenue for stratification of resource allocation. Put simply,
299 with one re-plan allowed, almost all patients would be best served via re-planning early during
300 treatment; however, as the budget of re-planning staff/technical/time resources expand, evidence-
301 based personalized re-planning is potentiated by our MDP approach.

302 **Data availability statement:** The anonymized data from the enclosed manuscript has been
303 deposited at DOI:10.6084/m9.figshare.25517338; a referee version is available for review at
304 <https://figshare.com/s/64bc3481737d17fc287e>.

305 **Preprint availability:** A preprint/pre-peer review version of the enclosed manuscript has been
306 submitted in accordance with NIH NOT-OD-17-050, “Reporting Preprints and Other Interim
307 Research Products” simultaneous with initial submission for peer-review and is available at
308 <https://doi.org/10.1101/2024.04.01.24305163>.

309 **Acknowledgment**

310 This work was supported by the National Institutes of Health (NIH) National Cancer Institute
311 (NCI) Research Grant (R01CA257814), the NCI Cancer Center Support Grant Program in Image-
312 Driven Biologically-informed Therapy (IDBT) Program (P30CA016672), and the Image Guided
313 Cancer Therapy Research Program at The University of Texas MD Anderson Cancer Center, and
314 the MD Anderson Charles and Dancien Stiefel Center for Head and Neck Cancer Oropharyngeal
315 Cancer Research Program. Lucas B. McCullum and Raul Garcia were supported by the NCI
316 Supplement program under R01CA257814-02S2, and R01CA257814-03S2, respectively. Drs.
317 McDonald and Wahid are both supported by the Image-guided Cancer Therapy T32 Fellowship
318 (T32CA261856). Dr. Heukelom received related support from the Netherlands Rene Vogels Fond
319 Fellowship. Drs. Heukelom and van Dijk received relevant support from the Dutch Cancer
320 Society/KWF Kankerbestrijding. Dr. Fuller received related support from the National Institute
321 of Dental and Craniofacial Research (NIDCR) (R01DE028290). Dr. Fuller has received related
322 direct industry grant/in-kind support, honoraria, and travel funding from Elekta AB. Dr. Fuller
323 has served in an unrelated consulting capacity for Varian/Siemens Healthineers, Philips Medical
324 Systems, and Oncospace, Inc. Dr. Brock received unrelated support from the Helen Black Image
325 Guided Fund, RaySearch Laboratories AB, the Apache Corporation, and the Tumor Measurement
326 Initiative through the MD Anderson Strategic Initiative Development Program (STRIDE) and various
327 NIH mechanisms. Dr. Scott received relevant support under the NCI Case Comprehensive
328 Cancer Center Support Grant (P30CA043703), with additional unrelated NIH support. Dr.
329 Moreno received related support from NIDCR (K01DE030524) and NCI (K12CA088084) during
330 the project period, with additional unrelated NIH support.

References

- [1] Iacovelli NA, et al. Role of IMRT/VMAT-based dose and volume parameters in predicting 5-year local control and survival in nasopharyngeal cancer patients. *Frontiers in Oncology* 2020;10:e518110.
- [2] Barker Jr JL, et al. Quantification of volumetric and geometric changes occurring during fractionated radiotherapy for head-and-neck cancer using an integrated CT/linear accelerator system. *International Journal of Radiation Oncology, Biology, Physics* 2004;59(4):960–70.
- [3] Beltran M, Ramos M, Rovira JJ, Perez-Hoyos S, Sancho M, Puertas E, Benavente S, Ginjaume M, Giralt J. Dose variations in tumor volumes and organs at risk during IMRT for head-and-neck cancer. *Journal of Applied Clinical Medical Physics* 2012;13(6):e3723.
- [4] Chen W, Bai P, Pan J, Xu Y, Chen K. Changes in tumor volumes and spatial locations relative to normal tissues during cervical cancer radiotherapy assessed by cone beam computed tomography. *Technology in Cancer Research and Treatment* 2017;16(2):246–52.
- [5] Beadle BM, Chan AW. The potential of adaptive radiotherapy for patients with head and neck cancer-too much or not enough? *JAMA Oncology* 2023; 9(8):1064–65.
- [6] Castelli J, Simon A, Lafond C, Perichon N, Rigaud B, Chajon E, De Bari B, Ozsahin M, Bourhis J, de Crevoisier R. Adaptive radiotherapy for head and neck cancer. *Acta Oncology* 2018;57(10):1284–92.
- [7] Figen M, Öksüz DÇ, Duman E, Prestwich R, Dyker K, Cardale K, Ramasamy S, Murray P, Şen M. Radiotherapy for head and neck cancer: Evaluation of triggered adaptive replanning in routine practice. *Frontiers in Oncology* 2020;59(4):960-70.
- [8] Håkansson K, Giannoulis E, Lindegaard A, Friberg J, Vogelius I. CBCT-based online adaptive radiotherapy for head and neck cancer-dosimetric evaluation of first clinical. *Acta Oncologica* 2023; 62(11):1369–1374.
- [9] Lavrova E, Garrett MD, Wang YF, Chin C, Elliston C, Savacool M, Price M, Kachnic LA, Horowitz DP. Adaptive radiation therapy: A review of CT-based techniques. *Radiology. Imaging Cancer* 2023; 5(4):e230011.
- [10] O’Hara CJ, Bird D, Al-Qaisieh B, Speight R. Assessment of CBCT-based synthetic CT generation accuracy for adaptive radiotherapy planning. *Journal of Applied Clinical Medical Physics* 2022; 23(11):e13737.
- [11] Brock KK. Adaptive radiotherapy: Moving into the future. *Seminars in Radiation Oncology* 2019; 29(3):181–184.
- [12] Wahid, KA et al. Harnessing uncertainty in radiotherapy auto-segmentation quality assurance. *Physics and Imaging in Radiation Oncology* 2023; 29:100526.
- [13] Allen C, Yeo AU, Hardcastle N, Franich RD. Evaluating synthetic computed tomography images for adaptive radiotherapy decision making in head and neck cancer. *Physics and Imaging in Radiation Oncology* 2023; 27:100478.
- [14] Taasti VT, et al. Clinical evaluation of synthetic computed tomography methods in adaptive

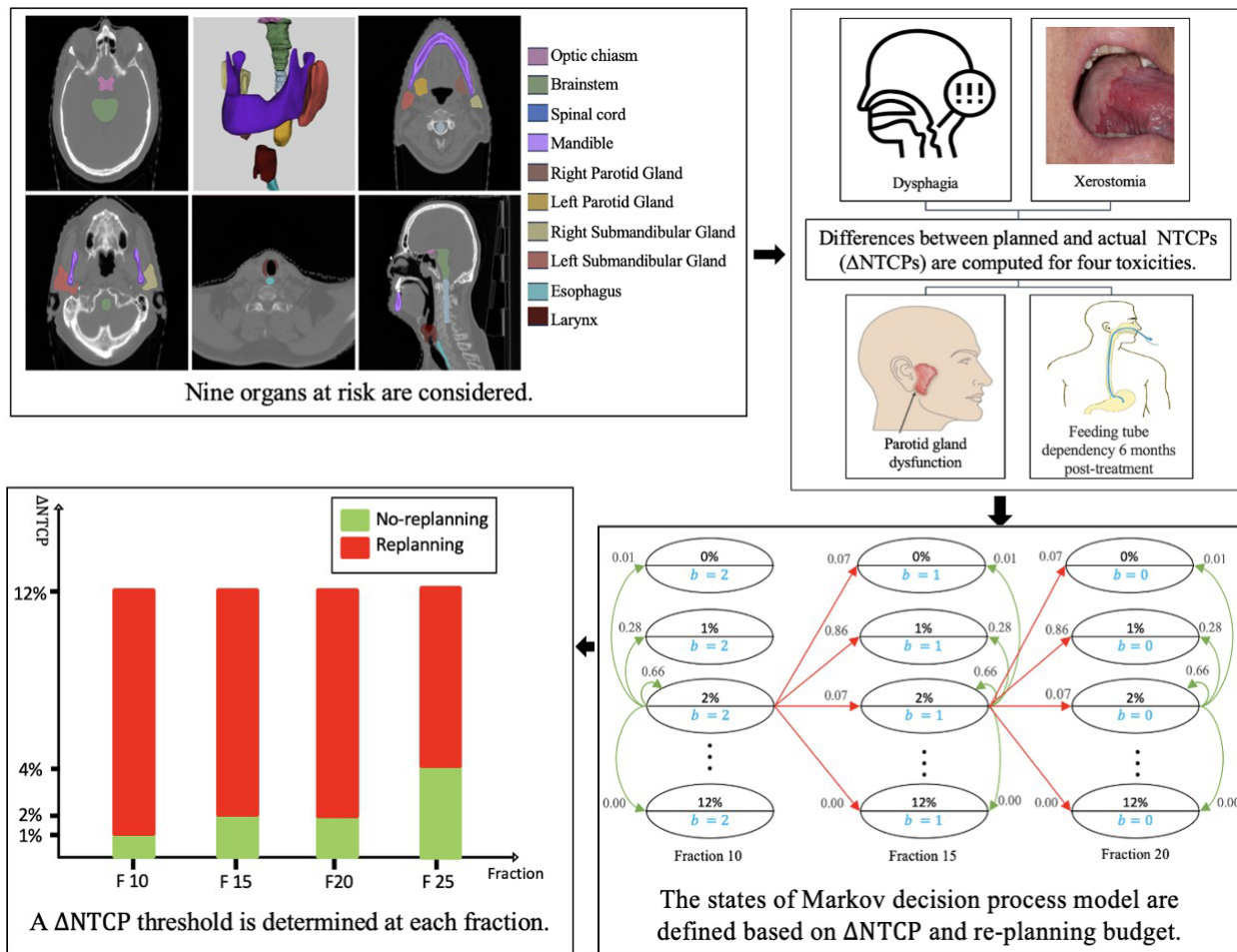
proton therapy of lung cancer patients. *Physics and Imaging in Radiation Oncology* 2023;27:e100459.

- [15] Huynh E, Hosny A, Guthier C, Bitterman SF, Hass-Kogan DA, Kann B, Aerts HJWL, Mak RG. Artificial intelligence in radiation oncology. *Nature Reviews Clinical Oncology* 2020; 17:771–81.
- [16] van de Schoot AJ, Hoffmans D, van Ingen KM, Simons MJ, Wiersma J. Characterization of Ethos therapy systems for adaptive radiation therapy: A multi- machine comparison. *Journal of Applied Clinical Medical Physics* 2023;24:e13905.
- [17] Varian Ethos. <https://www.varian.com>; 2024 [accessed 24 February 2024].
- [18] Avgousti R, Antypas C, Armpilia C, Simopoulou F, Liakouli Z, Karaiskos P, Kouloulas V, Kyrodimos E, Mouloupoulos LA, Zygianni A. Adaptive radiation therapy: When, how and what are the benefits that literature provides? *Cancer Radiotherapie: Journal de la Societe Francaise de Radiotherapie Oncologique* 2022;26(4):622–36.
- [19] Bahig H, et al. Magnetic resonance-based response assessment and dose adaptation in human papilloma virus positive tumors of the oropharynx treated with radiotherapy (MR-ADAPTOR): An R-IDEAL stage 2a-2b/Bayesian phase II trial. *Clinical and Translational Radiation Oncology* 2018;13:19–23.
- [20] Castelli J, et al. Weekly adaptive radiotherapy vs standard intensity-modulated radiotherapy for improving salivary function in patients with head and neck cancer: A phase 3 randomized clinical trial. *JAMA Oncology* 2023;9(8):1056–64.
- [21] Westerhoff JM, et al. Safety and tolerability of online adaptive high-field magnetic resonance-guided radiotherapy. *JAMA Network Open* 2024;7(5):e2410819.
- [22] Heukelom J, et al. Differences between planned and delivered dose for head and neck cancer, and their consequences for normal tissue complication probability and treatment adaptation. *Radiotherapy and Oncology* 2020;142:100–6.
- [23] Feinberg EA, Shwartz A. *Handbook of Markov Decision Processes: Methods and Applications*. New York: Springer; 2002.
- [24] Puterman ML. *Markov Decision Processes: Discrete Stochastic Dynamic Programming*. New York: Wiley-Interscience; 2005.
- [25] Beck JR, Pauker SG. The Markov process in medical prognosis. *Medical Decision Making* 1983;3(4):419–58.
- [26] Kuntz KM, Russell LB, Owens DK, Sanders GD, Trikalinos TA, Salomon JA. *Decision models in cost-effectiveness analysis. Cost-Effectiveness in Health and Medicine*. New York: Oxford University Press, 2016.
- [27] Ng SP et al. Surveillance imaging for patients with head and neck cancer treated with definitive radiotherapy: A partially observed Markov decision process model. *Cancer* 2020;126(4):749–56.
- [28] Alagoz O, Hsu H, Schaefer AJ, Roberts MS. Markov decision processes: A tool for sequential decision making under uncertainty. *Medical Decision Making: An International Journal of the Society for Medical Decision Making* 2010;30(4):474–83.
- [29] Alagoz O, Maillart LM, Schaefer AJ, Roberts MS. The optimal timing of living-donor liver transplantation. *Management Science* 2004;50(10):1420–30.

- [30] Denton BT, Kurt M, Shah ND, Bryant SC, Smith SA. Optimizing the start time of statin therapy for patients with diabetes. *Medical Decision Making* 2009;29(3):351–67.
- [31] Shechter SM, Bailey MD, Schaefer AJ, Roberts MS. The optimal time to initiate HIV therapy under ordered health states. *Operations Research* 2008;56(1):20–33.
- [32] MATLAB version: 9.13.0 (R2022b), Natick, Massachusetts: The MathWorks Inc.; 2022.
- [33] Zhang L, Dong L, Court L, Wang H, Gillin M, Mohan R. TU-EE-A4-05: Validation of CT-assisted targeting (CAT) software for soft tissue and bony target localization. *Medical Physics* 2005;32:2106.
- [34] Maki RG, et al. Phase II study of sorafenib in patients with metastatic or recurrent sarcomas. *Journal of Clinical Oncology: Official Journal of the American Society of Clinical Oncology* 2009;27(19):3133–40.
- [35] Stieb S, Lee A, van Dijk LV, Frank S, Fuller CD, Blanchard P. NTCP modeling of late effects for head and neck cancer: A systematic review. *International Journal of Particle Therapy* 2021;8(1):95–107.
- [36] Hosseinian S, Hemmati M, Dede C, Salzillo TC, van Dijk LV, Mohamed ASR, Lai SY, Schaefer AJ, Fuller CD. Cluster-based toxicity estimation of osteoradionecrosis via unsupervised machine learning: Moving beyond single dose-parameter normal tissue complication probability by using whole dose-volume histograms for cohort risk stratification. *International Journal of Radiation Oncology, Biology, Physics* 2024;119(5):1569–78.
- [37] American Cancer Society. Head and Neck Cancer: Statistics. <https://www.cancer.net/cancer-types/head-and-neck-cancer/statistics>; 2024 [accessed 24 February 2024].
- [38] Gan Y, Langendijk JA, van der Schaaf A, van den Bosch L, Oldehinkel E, Lin Z, Both S, Brouwer CL. An efficient strategy to select head and neck cancer patients for adaptive radiotherapy. *Radiotherapy and Oncology: Journal of the European Society for Therapeutic Radiology and Oncology* 2023;186:e109763.
- [39] Gan Y, Langendijk JA, Oldehinkel E, Lin Z, Both S, Brouwer CL. Optimal timing of re-planning for head and neck adaptive radiotherapy. *Journal of the European Society for Therapeutic Radiology and Oncology* 2024;194:e110145.
- [40] Heukelom J, et al. Adaptive and innovative radiation treatment for improving cancer treatment outcome (ARTFORCE); a randomized controlled phase II trial for individualized treatment of head and neck cancer. *BMC Cancer* 2013;13:84.
- [41] Leeuw AD, et al. Acute toxicity in ARTFORCE: A randomized phase III dose-painting trial in head and neck cancer. *International Journal of Radiation Oncology, Biology, Physics* 2022;114(3):S98.
- [42] Mohamad I, et al. The evolving role of stereotactic body radiation therapy for head and neck cancer: Where do we stand? *Cancers (Basel)* 2023;15(20):e5010.
- [43] Lalonde A, Bobić M, Sharp GC, Chamseddine I, Winey B, Paganetti H. Evaluating the effect of setup uncertainty reduction and adaptation to geometric changes on normal tissue complication probability using online adaptive head and neck intensity modulated proton therapy. *Physics in*

Medicine and Biology 2023;68(11):e115018.

- [44] Yap LM, Jamalludin Z, Ng AH, Ung NM. A multi-center survey on adaptive radiation therapy for head and neck cancer in Malaysia. *Physical and Engineering Sciences in Medicine* 2023;46(3):1331–40.
- [45] Bertholet J, et al. Patterns of practice for adaptive and real-time radiation therapy (POP-ART RT) part II: Offline and online plan adaption for interfractional changes. *Radiotherapy and Oncology: Journal of the European Society for Therapeutic Radiology and Oncology* 2020;153:88–96.



Graphical Abstract: Overview of the analysis method. The sub-figures displaying Organs at risk and toxicities are adapted from [1] with permission. Abbreviation: NTCP = Normal tissue complications probability.

References

- [1] Fuller CD. Introduction to Radiation Oncology, <https://doi.org/10.6084/m9.figshare.22582207.v1>; 2023 [accessed 24 February 2024].

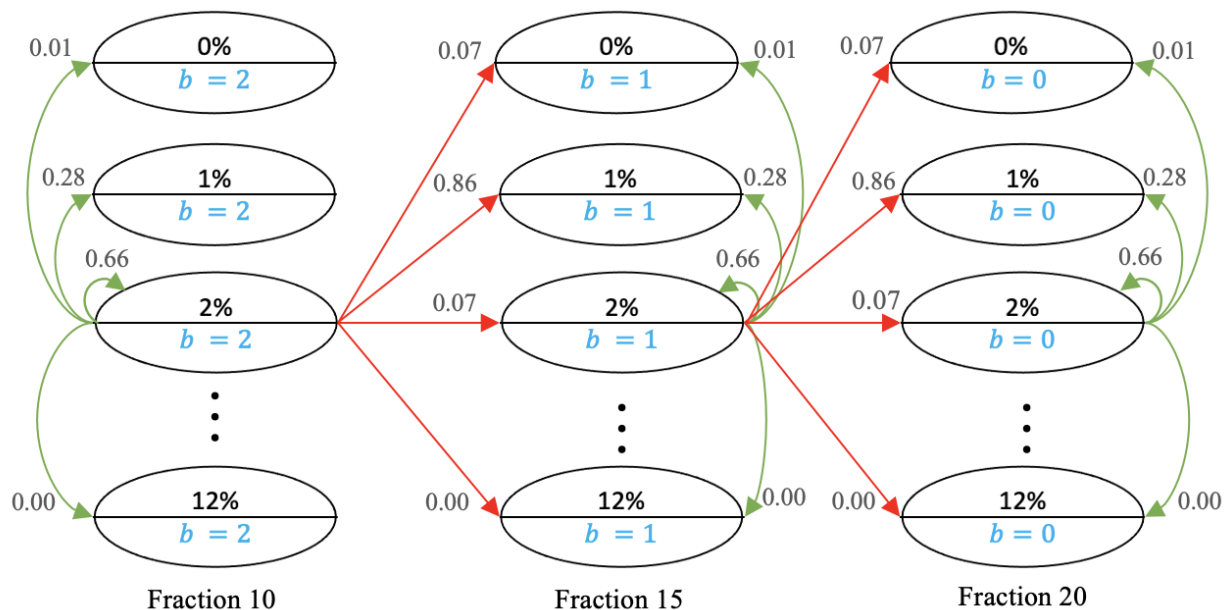


Fig. 1: Markov Decision Process Model. The permissible number of re-plans is 2 ($B = 2$). The states are shown by ellipses. Δ NTCP values are located in the upper half of the ellipses, while the lower halves contain the value of b (the number of remaining re-plans). Transitions between states are shown by green arrows when the action is 'no re-planning' and by red arrows when the action is 're-planning.' Not all arrows, states, and fractions are included to avoid ambiguity. For example, the smoothed transition probability from state (2%,2) state to (1%,1) when the action is 're-planning' is 0.86.

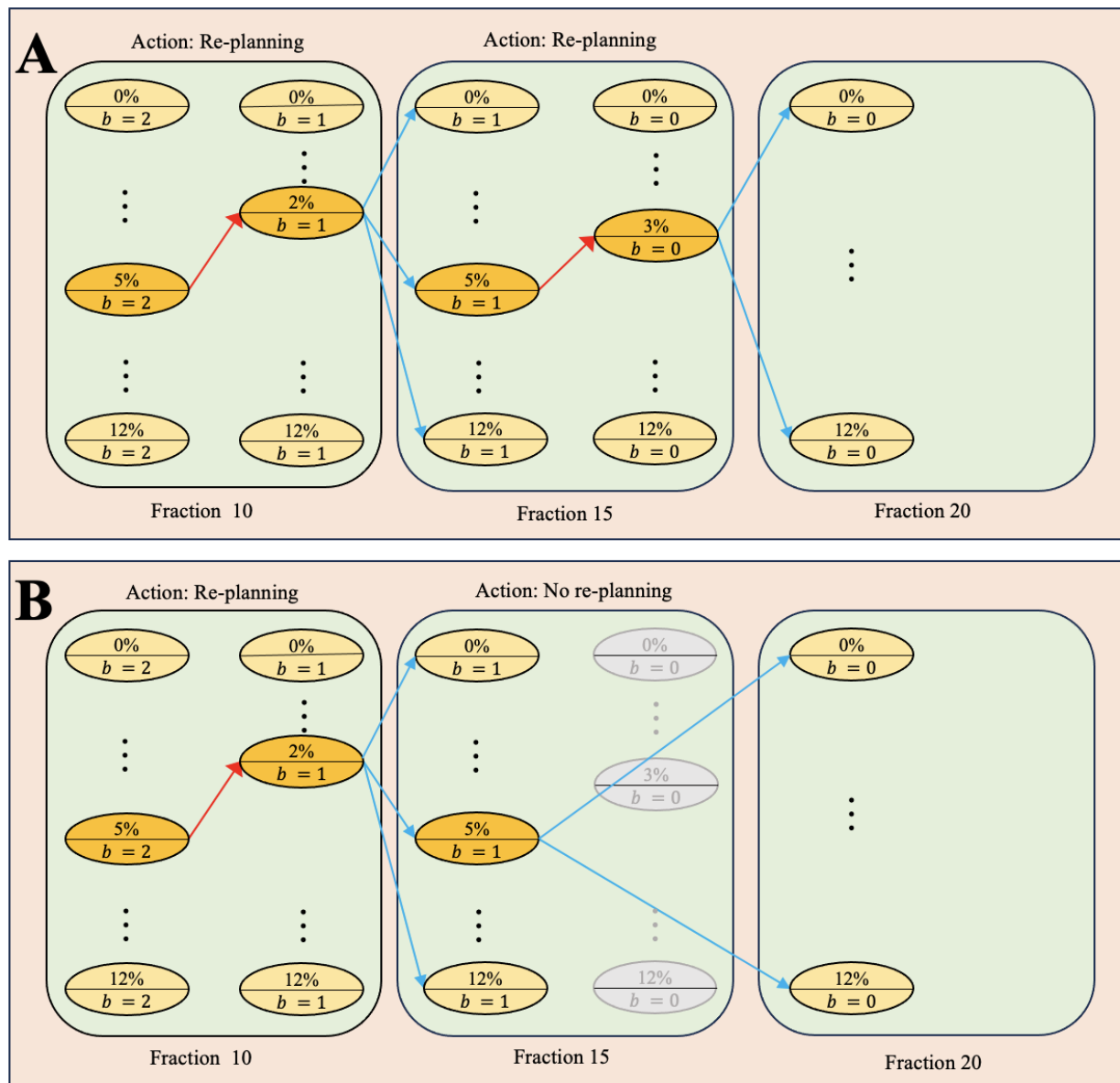


Fig. 2: Effect of actions on system transitions. The permissible number of re-plans is 2 ($B = 2$). The states are represented by ellipses. The ΔNTCP values are located in the upper halves of the ellipses, while the lower halves contain the value of b (the number of remaining re-plans). When the action at a fraction is ‘re-planning,’ as in Fractions 10 and 15 in Part A and Fraction 10 in Part B, the transition to a state with a lower ΔNTCP within the same fraction is shown with red arrows. Transitions between states from one fraction to the next are shown with blue arrows. When the action is ‘no re-planning,’ as in Fraction 15 in Part B, no transition occurs within that fraction. Instead, the system transitions to a new state at Fraction 20. This is depicted by the gray states at Fraction 15, indicating that there is no immediate decrease in ΔNTCP .

Supplementary Material A. Literature Review on Head-and-neck-cancer Adaptive Radiation Therapy.

Table A1: A comprehensive list of relevant papers on head-and-neck-cancer ART along with the number of re-plan and the reported fractions.

Paper	Replan Trigger	Replan Frequency
Castelli et al. [1]	None	Replan weekly
Lim et al. [2]	Parotid dose	Replan at F14
McDonald et al. [3]	Weight loss or	Case studies of replans on four patients, one at F6, F8, F24, F26
Reinders et al. [4]	None	Replan weekly
Kee et al. [5]	Tumor ADC	Replan at week 2 and 4, Increase dose at F10
Ciarmatori et al. [6]	None	Single replan at F18
Maffei et al. [7]	None	Optimal replan at F18
Wang et al. [8]	None	Single replan at F18
Gros et al. [9]	Dosimetric factors	Optimal replan between F1 and F23
Duma et al. [10]	Weight loss	Replan varied from F6 to F20
Fung et al. [11]	None	Replan after F25 and F35
Kuo et al. [12]	None	Replan after F25
Hansen et al. [13]	Weight loss or tumor shrinkage	Replan after $F19 \pm 6$
Capelle et al. [14]	None	Replan at F20
Brwon et al. [15]	Source-to-skin distance corrections	Median re-planning at F22 and F26
Castelli et al. [16]	None	Replan weekly
Brown et al. [17]	Nodal volume	Median re-planning at F11 for nasopharyngeal and at F20 for oropharyngeal
Aly et al. [18]	None	Replan weekly
Figen et al. [19]	Weight loss or tumor shrinkage	Mean replan at F15
Bobić et al. [20]	None	Replan weekly
Gupta et al. [21]	None	Replan daily

Supplementary Material B. Patient Characteristics.

Table B1: Patient characteristics. Abbreviations: cCRT = concurrent chemoradiation. RT = radiotherapy. TNM classification according to version 3. Accelerated RT: 2 Gy per fraction, 6 times per week.

Variable	Number of Patients = 52	Percentage
Sex	Male	69%
	Female	31%
Age	18-65 years	88%
	≥ 65 years	12%
T-classification	Tis-T1	8%
	T2	15%
	T3	13%
	T4	54%
	Recurrence	8%
	Unknown	2%
	Post-surgery	23%
N-classification	N0	27%
	N1	19%
	N2	38%
	N3	2%
Primary site	Larynx	2%
	Oropharynx	25%
	Oral cavity	8%
	Hypopharynx	0%
	Nasopharynx	29%
	Sinonasal	23%
Pathology	Adenocarcinoma	2%
	Neuroblastoma	6%
	Neuroendocrine	8%
	Squamous cell carcinoma	50%
	Undifferentiated carcinoma	17%
	Other	17%
	Treatment modality	Radiotherapy alone
Induction chemotherapy followed by RT	4%	
Induction chemotherapy followed by cCRT	31%	
Concurrent chemoradiation	27%	
Radiation + Cetuximab	8%	
Baseline weight loss	No weight loss	38%
	Moderate weight loss (1 – 10%)	33%
	Severe weight loss (>10%)	6%
	Unknown	23%
Baseline xerostomia	No xerostomia	4%
	Some xerostomia	8%
	Unknown	88%
Accelerated RT	Yes	6%

Supplementary Material C. Transition Probabilities.

Action 1: No re-planning

The natural transition probabilities from fraction 0 (pre-treatment) to fraction 10 were directly estimated using the information provided in Table 1. For each Δ NTCP category, the ratio of the corresponding number of patients at fraction 10 to the total of 52 patients was taken as the associated transition probability. We note that all patients exhibit Δ NTCP = 0% at fraction 0. These probabilities apply only to the states with the same number of remaining re-plans b , by the definition of the ‘no re-planning’ action. The transition probabilities are presented in Supplementary Table C1.

Table C1: Transition probabilities from fraction 0 (F0) to fraction 10 (F10) under ‘no re-planning.’

Δ NTCP @ F10 → Δ NTCP @ F0 ↓	0%	1%	2%	3%	4%	5%	6%	7%	8%	9%	10%	11%	12%
0%	0.50	0.13	0.08	0.11	0.04	0.04	0.00	0.02	0.00	0.00	0.02	0.02	0.04

The natural transition probabilities from fraction 10 to fraction 15 were estimated in a similar manner. As the number of patients in each Δ NTCP category at fraction 15 were aggregated, a mapping from Δ NTCP categories at fraction 10 to those of fraction 15 was established. To ensure a feasible map, it was assumed that Δ NTCPs may slightly improve (1%) on its own, without intervention. The necessity of this assumption may be observed by the number of patients with Δ NTCP = 12% at Fraction 10 and 15 in Table 1; two patients exhibited Δ NTCP = 12% at fraction 10, while this number at fraction 15 was one patient. As no patient showed Δ NTCP = 6%, 8%, 9% at fraction 10, it was assumed that the patients in these categories retain the same Δ NTCP at fraction 15 with probability 1. The transition probabilities are presented in Supplementary Table C2.

Table C2: Transition probabilities from fraction 10 (F10) to fraction 15 (F15) under ‘no re-planning.’ The same probabilities apply to subsequent transitions, i.e., from F15 to F20, from F20 to F25, and from F25 to end-treatment, under ‘no re-planning.’

Δ NTCP @ F15 → Δ NTCP @ F10 ↓	0%	1%	2%	3%	4%	5%	6%	7%	8%	9%	10%	11%	12%
0%	0.88	0.00	0.12	0.00	0.00	0.00	0.00	0.00	0.00	0.00	0.00	0.00	0.00
1%	0.00	1.00	0.00	0.00	0.00	0.00	0.00	0.00	0.00	0.00	0.00	0.00	0.00
2%	0.00	0.25	0.75	0.00	0.00	0.00	0.00	0.00	0.00	0.00	0.00	0.00	0.00
3%	0.00	0.00	0.50	0.33	0.17	0.00	0.00	0.00	0.00	0.00	0.00	0.00	0.00
4%	0.00	0.00	0.00	0.00	0.50	0.00	0.50	0.00	0.00	0.00	0.00	0.00	0.00
5%	0.00	0.00	0.00	0.00	0.00	0.50	0.00	0.50	0.00	0.00	0.00	0.00	0.00
6%	0.00	0.00	0.00	0.00	0.00	0.00	1.00	0.00	0.00	0.00	0.00	0.00	0.00
7%	0.00	0.00	0.00	0.00	0.00	0.00	0.00	1.00	0.00	0.00	0.00	0.00	0.00
8%	0.00	0.00	0.00	0.00	0.00	0.00	0.00	0.00	1.00	0.00	0.00	0.00	0.00
9%	0.00	0.00	0.00	0.00	0.00	0.00	0.00	0.00	0.00	1.00	0.00	0.00	0.00
10%	0.00	0.00	0.00	0.00	0.00	0.00	0.00	0.00	0.00	0.00	1.00	0.00	0.00
11%	0.00	0.00	0.00	0.00	0.00	0.00	0.00	0.00	0.00	0.00	0.00	1.00	0.00
12%	0.00	0.00	0.00	0.00	0.00	0.00	0.00	0.00	0.00	0.00	0.00	0.00	0.50 0.50

Table C3: Smoothed Transition probabilities from fraction 10 (F10) to fraction 15 (F15) under ‘no re-planning.’ The same probabilities apply to subsequent transitions, i.e., from F15 to F20, from F20 to F25, and from F25 to end-treatment, under ‘no re-planning.’

$\Delta\text{NTCP @ F15} \rightarrow$ $\Delta\text{NTCP @ F10} \downarrow$	0%	1%	2%	3%	4%	5%	6%	7%	8%	9%	10%	11%	12%
0%	0.81	0.08	0.11	0.00	0.00	0.00	0.00	0.00	0.00	0.00	0.00	0.00	0.00
1%	0.07	0.86	0.07	0.00	0.00	0.00	0.00	0.00	0.00	0.00	0.00	0.00	0.00
2%	0.01	0.28	0.66	0.04	0.01	0.00	0.00	0.00	0.00	0.00	0.00	0.00	0.00
3%	0.00	0.03	0.46	0.31	0.17	0.01	0.02	0.00	0.00	0.00	0.00	0.00	0.00
4%	0.00	0.00	0.02	0.03	0.43	0.06	0.42	0.04	0.00	0.00	0.00	0.00	0.00
5%	0.00	0.00	0.00	0.00	0.04	0.43	0.09	0.42	0.02	0.00	0.00	0.00	0.00
6%	0.00	0.00	0.00	0.00	0.00	0.06	0.85	0.09	0.00	0.00	0.00	0.00	0.00
7%	0.00	0.00	0.00	0.00	0.00	0.00	0.07	0.85	0.08	0.00	0.00	0.00	0.00
8%	0.00	0.00	0.00	0.00	0.00	0.00	0.00	0.07	0.85	0.08	0.00	0.00	0.00
9%	0.00	0.00	0.00	0.00	0.00	0.00	0.00	0.00	0.07	0.85	0.08	0.00	0.00
10%	0.00	0.00	0.00	0.00	0.00	0.00	0.00	0.00	0.00	0.08	0.88	0.04	0.00
11%	0.00	0.00	0.00	0.00	0.00	0.00	0.00	0.00	0.00	0.04	0.88	0.06	0.02
12%	0.00	0.00	0.00	0.00	0.00	0.00	0.00	0.00	0.00	0.00	0.06	0.46	0.48

Action 2: Re-planning

The impact of ‘re-planning’ on transition probabilities at a specific fraction was modeled by presuming an immediate reduction in ΔNTCP to a proportion relative to the elapsed treatment time, followed by a natural transition governed by the probabilities associated with the reduced ΔNTCP . For instance, ‘re-planning’ at fraction 10 when ΔNTCP is at 5% results in an immediate decrease to $\Delta\text{NTCP} = 2\%$, reflecting that about one-third of the treatment has been completed. This is then followed by a transition (from F10 to F15) according to the probabilities associated with $\Delta\text{NTCP} = 2\%$ @ F10 in Supplementary Table C2. These probabilities are presented in the following tables. We note that the earliest decision epoch for ‘re-planning’ is fraction 10.

Table C4: Transition probabilities from fraction 10 (F10) to fraction 15 (F15) under ‘re-planning.’

$\Delta\text{NTCP @ F15} \rightarrow$ $\Delta\text{NTCP @ F10} \downarrow$	0%	1%	2%	3%	4%	5%	6%	7%	8%	9%	10%	11%	12%
0%	0.81	0.08	0.11	0.00	0.00	0.00	0.00	0.00	0.00	0.00	0.00	0.00	0.00
1%	0.81	0.08	0.11	0.00	0.00	0.00	0.00	0.00	0.00	0.00	0.00	0.00	0.00
2%	0.07	0.86	0.07	0.00	0.00	0.00	0.00	0.00	0.00	0.00	0.00	0.00	0.00
3%	0.07	0.86	0.07	0.00	0.00	0.00	0.00	0.00	0.00	0.00	0.00	0.00	0.00
4%	0.07	0.86	0.07	0.00	0.00	0.00	0.00	0.00	0.00	0.00	0.00	0.00	0.00
5%	0.01	0.28	0.66	0.04	0.01	0.00	0.00	0.00	0.00	0.00	0.00	0.00	0.00
6%	0.01	0.28	0.66	0.04	0.01	0.00	0.00	0.00	0.00	0.00	0.00	0.00	0.00
7%	0.01	0.28	0.66	0.04	0.01	0.00	0.00	0.00	0.00	0.00	0.00	0.00	0.00
8%	0.00	0.03	0.46	0.31	0.17	0.01	0.02	0.00	0.00	0.00	0.00	0.00	0.00
9%	0.00	0.03	0.46	0.31	0.17	0.01	0.02	0.00	0.00	0.00	0.00	0.00	0.00
10%	0.00	0.03	0.46	0.31	0.17	0.01	0.02	0.00	0.00	0.00	0.00	0.00	0.00
11%	0.00	0.00	0.02	0.03	0.43	0.06	0.42	0.04	0.00	0.00	0.00	0.00	0.00
12%	0.00	0.00	0.02	0.03	0.43	0.06	0.42	0.04	0.00	0.00	0.00	0.00	0.00

Table C5: Transition probabilities from fraction 15 (F15) to fraction 20 (F20) under ‘re-planning.’

Δ NTCP @ F20 → Δ NTCP @ F15 ↓	0%	1%	2%	3%	4%	5%	6%	7%	8%	9%	10%	11%	12%
0%	0.81	0.08	0.11	0.00	0.00	0.00	0.00	0.00	0.00	0.00	0.00	0.00	0.00
1%	0.07	0.86	0.07	0.00	0.00	0.00	0.00	0.00	0.00	0.00	0.00	0.00	0.00
2%	0.07	0.86	0.07	0.00	0.00	0.00	0.00	0.00	0.00	0.00	0.00	0.00	0.00
3%	0.01	0.28	0.66	0.04	0.01	0.00	0.00	0.00	0.00	0.00	0.00	0.00	0.00
4%	0.01	0.28	0.66	0.04	0.01	0.00	0.00	0.00	0.00	0.00	0.00	0.00	0.00
5%	0.00	0.03	0.46	0.31	0.17	0.01	0.02	0.00	0.00	0.00	0.00	0.00	0.00
6%	0.00	0.03	0.46	0.31	0.17	0.01	0.02	0.00	0.00	0.00	0.00	0.00	0.00
7%	0.00	0.00	0.02	0.03	0.43	0.06	0.42	0.04	0.00	0.00	0.00	0.00	0.00
8%	0.00	0.00	0.02	0.03	0.43	0.06	0.42	0.04	0.00	0.00	0.00	0.00	0.00
9%	0.00	0.00	0.00	0.00	0.04	0.43	0.09	0.42	0.02	0.00	0.00	0.00	0.00
10%	0.00	0.00	0.00	0.00	0.04	0.43	0.09	0.42	0.02	0.00	0.00	0.00	0.00
11%	0.00	0.00	0.00	0.00	0.00	0.06	0.85	0.09	0.00	0.00	0.00	0.00	0.00
12%	0.00	0.00	0.00	0.00	0.00	0.06	0.85	0.09	0.00	0.00	0.00	0.00	0.00

Table C6: Transition probabilities from fraction 20 (F20) to fraction 25 (F25) under ‘re-planning.’

Δ NTCP @ F25 → Δ NTCP @ F20 ↓	0%	1%	2%	3%	4%	5%	6%	7%	8%	9%	10%	11%	12%
0%	0.81	0.08	0.11	0.00	0.00	0.00	0.00	0.00	0.00	0.00	0.00	0.00	0.00
1%	0.07	0.86	0.07	0.00	0.00	0.00	0.00	0.00	0.00	0.00	0.00	0.00	0.00
2%	0.07	0.86	0.07	0.00	0.00	0.00	0.00	0.00	0.00	0.00	0.00	0.00	0.00
3%	0.01	0.28	0.66	0.04	0.01	0.00	0.00	0.00	0.00	0.00	0.00	0.00	0.00
4%	0.00	0.03	0.46	0.31	0.17	0.01	0.02	0.00	0.00	0.00	0.00	0.00	0.00
5%	0.00	0.03	0.46	0.31	0.17	0.01	0.02	0.00	0.00	0.00	0.00	0.00	0.00
6%	0.00	0.00	0.02	0.03	0.43	0.06	0.42	0.04	0.00	0.00	0.00	0.00	0.00
7%	0.00	0.00	0.00	0.00	0.04	0.43	0.09	0.42	0.02	0.00	0.00	0.00	0.00
8%	0.00	0.00	0.00	0.00	0.04	0.43	0.09	0.42	0.02	0.00	0.00	0.00	0.00
9%	0.00	0.00	0.00	0.00	0.00	0.06	0.85	0.09	0.00	0.00	0.00	0.00	0.00
10%	0.00	0.00	0.00	0.00	0.00	0.00	0.07	0.85	0.08	0.00	0.00	0.00	0.00
11%	0.00	0.00	0.00	0.00	0.00	0.00	0.07	0.85	0.08	0.00	0.00	0.00	0.00
12%	0.00	0.00	0.00	0.00	0.00	0.00	0.00	0.07	0.85	0.08	0.00	0.00	0.00

Table C7: Transition probabilities from fraction 25 (F25) to end-treatment under ‘re-planning.’

Δ NTCP @ end → Δ NTCP @ F25 ↓	0%	1%	2%	3%	4%	5%	6%	7%	8%	9%	10%	11%	12%
0%	0.81	0.08	0.11	0.00	0.00	0.00	0.00	0.00	0.00	0.00	0.00	0.00	0.00
1%	0.07	0.86	0.07	0.00	0.00	0.00	0.00	0.00	0.00	0.00	0.00	0.00	0.00
2%	0.01	0.28	0.66	0.04	0.01	0.00	0.00	0.00	0.00	0.00	0.00	0.00	0.00
3%	0.00	0.03	0.46	0.31	0.17	0.01	0.02	0.00	0.00	0.00	0.00	0.00	0.00
4%	0.00	0.03	0.46	0.31	0.17	0.01	0.02	0.00	0.00	0.00	0.00	0.00	0.00
5%	0.00	0.00	0.02	0.03	0.43	0.06	0.42	0.04	0.00	0.00	0.00	0.00	0.00
6%	0.00	0.00	0.00	0.00	0.04	0.43	0.09	0.42	0.02	0.00	0.00	0.00	0.00
7%	0.00	0.00	0.00	0.00	0.00	0.06	0.85	0.09	0.00	0.00	0.00	0.00	0.00
8%	0.00	0.00	0.00	0.00	0.00	0.00	0.07	0.85	0.08	0.00	0.00	0.00	0.00
9%	0.00	0.00	0.00	0.00	0.00	0.00	0.00	0.07	0.85	0.08	0.00	0.00	0.00
10%	0.00	0.00	0.00	0.00	0.00	0.00	0.00	0.07	0.85	0.08	0.00	0.00	0.00
11%	0.00	0.00	0.00	0.00	0.00	0.00	0.00	0.00	0.07	0.85	0.08	0.00	0.00
12%	0.00	0.00	0.00	0.00	0.00	0.00	0.00	0.00	0.00	0.08	0.88	0.04	0.00

Supplementary Material D. Optimal Δ NTCP Thresholds for Re-planning.

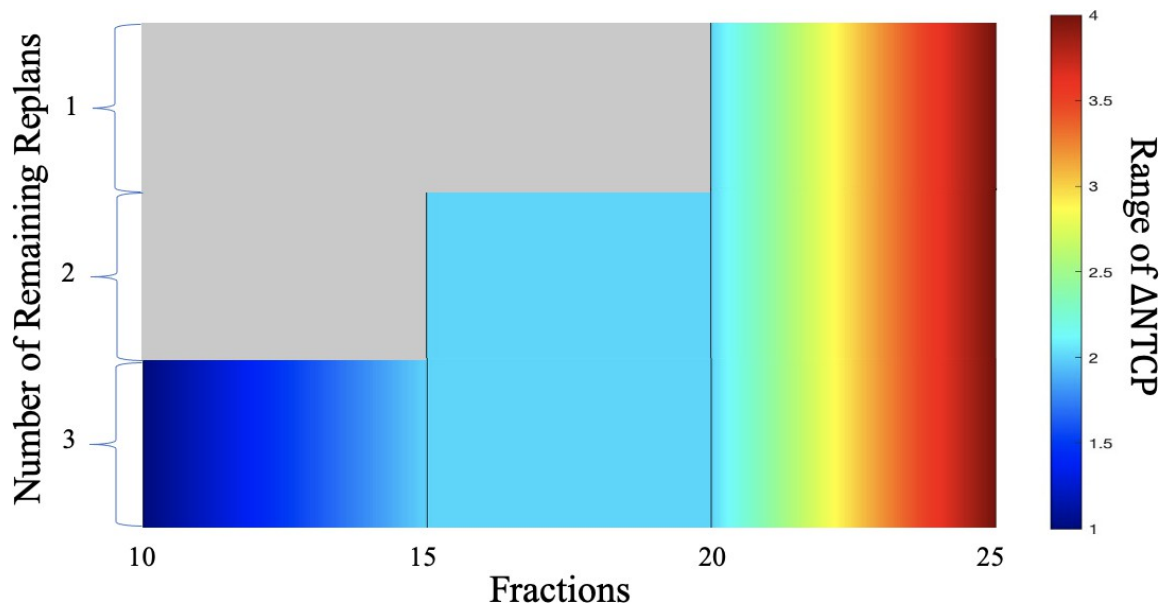


Fig. D1: Optimal Δ NTCP thresholds for re-planning for $B = 3$. Optimal Δ NTCP thresholds for re-planning at fractions 10, 15, 20, and 25 are 1%, 2%, 2%, and 4%, respectively. The optimal Δ NTCP thresholds increase with respect to fraction but remain constant with respect to the number of replans remaining.

Supplementary Material E. NTCP Models.

Table E1: The employed NTCP models for xerostomia, dysphagia, parotid gland dysfunction, and feeding tube dependency at 6 months post-treatment.

1. NTCP model for moderate to severe xerostomia at 6 months [22].

NTCP = $(1 + e^{-S})^{-1}$, where

$S = -1.443 + (\text{mean dose to contralateral parotid} * 0.047) + (\text{baseline xerostomia score} * 0.720)$. Baseline xerostomia is 0 (none) or 1 (a bit).

2. NTCP model for physician rated feeding tube dependency at 6 months [23]

NTCP = $(1 + e^{-S})^{-1}$, where

$S = -11.70 + (\text{advanced T-stage} * 0.43) + (\text{moderate weight loss} * 0.95) + (\text{severe weight loss} * 1.63) + (\text{accelerated radiotherapy} * 1.20) + (\text{chemoradiation} * 1.91) + (\text{radiotherapy plus cetuximab} * 0.56) + (\text{mean dose PCM superior} * 0.071) + (\text{mean dose PCM inferior} * 0.034) + (\text{mean dose contralateral parotid} * 0.006) + (\text{mean dose cricopharyngeal muscle} * 0.023)$.

The dose variables are in Gy, and for all the other variables 0 (no) or 1 (yes) are filled in.

3. NTCP model for physician rated decreased salivary flow using the mean dose model [24–26].

NTCP = $\frac{1}{\sqrt{2\pi}} \int_{-\infty}^u e^{-\frac{t^2}{2}} dt$, where $u = \frac{D - TD_{50}}{mTD_{50}}$

D is the mean parotid dose, TD_{50} is the dose resulting in 50% complication probability and m determines the slope of the model. The employed parameters were $TD_{50}=39.9$ Gy and $m = 0.4$.

4. NTCP model for dysphagia (grade 2–4 swallowing dysfunction according to the RTOG/EORTC Late Radiation Morbidity Scoring Criteria, physician rated 6 months after treatment) [27].

NTCP = $(1 + e^{-S})^{-1}$, where

$S = -6.09 + (\text{mean dose PCM superior} * 0.057) + (\text{mean dose supraglottic larynx} * 0.037)$.

References

- [1] Castelli J, et al. Weekly adaptive radiotherapy vs standard intensity-modulated radiotherapy for improving salivary function in patients with head and neck cancer: A phase 3 randomized clinical trial. *JAMA Oncology* 2023;9(8):1056–64.
- [2] Lim SY, Tran A, Tran ANK, Sobremonte A, Fuller CD, Simmons L, Yang J. Dose accumulation of daily adaptive plans to decide optimal plan adaptation strategy for head-and-neck patients treated with MR-Linac. *Medical Dosimetry: Official Journal of the American Association of Medical Dosimetrists* 2022;47(1):103–9.
- [3] McDonald BA, et al. Initial feasibility and clinical implementation of daily MR- guided adaptive head and neck cancer radiation therapy on a 1.5T MR-Linac system: Prospective R-IDEAL 2a/2b systematic clinical evaluation of technical innovation. *International Journal of Radiation Oncology, Biology, Physics* 2021;109(5):1606–18.
- [4] Reinders FCJ, de Ridder M, Doornaert PAH, Raaijmakers CPJ, Philippens MEP. Individual elective lymph node irradiation for the reduction of complications in head and neck cancer patients (iNode): A phase-I feasibility trial protocol. *Clinical and Translational Radiation Oncology* 2022;39:e100574.
- [5] H. Kee, et al. Optimising radiation therapy in head and neck cancers using functional image-guided radiotherapy and novel biomarkers. <https://clinicaltrials.gov/study/NCT04242459>; 2021 [accessed 16 September 2024].
- [6] Ciarmatori A, Maffei N, Mistretta GM, Ceroni P, Bernabei A, Meduri B, D’Angelo E, Bruni A, Giacobazzi P, Lohr F, Guidi G. Evaluation of the effectiveness of novel single-intervention adaptive radiotherapy strategies based on daily dose accumulation. *Medical Dosimetry: Official Journal of the American Association of Medical Dosimetrists* 2019;44(4):379–84.
- [7] Maffei N, et al. SIS epidemiological model for adaptive RT: Forecasting the parotid glands shrinkage during tomotherapy treatment. *Medical physics* 2016;43(7):e4294.
- [8] X. Wang, J. Lu, X. Xiong, G. Zhu, H. Ying, S. He, W. Hu, and C. Hu. Anatomic and dosimetric changes during the treatment course of intensity-modulated radiotherapy for locally advanced nasopharyngeal carcinoma. *Medical Dosimetry: Official Journal of the American Association of Medical Dosimetrists* 2010;35(2):151–7.
- [9] Gros SAA, Santhanam AP, Block AM, Emami B, Lee BH, Joyce C. Retrospective clinical evaluation of a decision-support software for adaptive radiotherapy of head and neck cancer patients. *Frontiers in Oncology* 2022;12:e777793.
- [10] Duma MN, Kampfer S, Schuster T, Winkler C, Geinitz H. Adaptive radiotherapy for soft tissue changes during helical tomotherapy for head and neck cancer. *Strahlentherapie und Onkologie* 2012;188(3):243–7.
- [11] Fung WW, Wu VW, Teo PM. Dosimetric evaluation of a three-phase adaptive radiotherapy for nasopharyngeal carcinoma using helical tomotherapy. *Medical Dosimetry: Official Journal of the American Association of Medical Dosimetrists* 2012;37(1):92–7.
- [12] Kuo YC, Wu TH, Chung TS, Huang KW, Chao KS, Su WC, Chiou JF. Effect of regression of enlarged neck lymph nodes on radiation doses received by parotid glands during intensity-modulated radiotherapy for head and neck cancer. *American Journal of Clinical Oncology* 2006;29(6):600–5.
- [13] Hansen EK, Bucci MK, Quivey JM, Weinberg V, Xia P. Repeat CT imaging and replanning during the course of IMRT for head-and-neck cancer. *International Journal of Radiation Oncology, Biology, Physics* 2006;64(2):355–62.

- [14] Capelle L, Mackenzie M, Field C, Parliament M, Ghosh S, Scrimger R. Adaptive radiotherapy using helical tomotherapy for head and neck cancer in definitive and postoperative settings: Initial results. *Clinical Oncology (Royal College of Radiologists (Great Britain))* 2012;24(3):208–15.
- [15] Brown E, Porceddu S, Owen R, Harden F. Developing an adaptive radiotherapy technique for virally mediated head and neck cancer. *Journal of Medical Imaging and Radiation Sciences* 2013;44(3):134–40.
- [16] Castelli J, et al. Impact of head and neck cancer adaptive radiotherapy to spare the parotid glands and decrease the risk of xerostomia. *Radiation Oncology* 2015;10(6).
- [17] Brown E, Owen R, Harden F, Mengersen K, Oestreich K, Houghton W, Poulsen M, Harris S, Lin C, Porceddu S. Head and neck adaptive radiotherapy: Predicting the time to replan. *Asia-Pacific Journal of Clinical Oncology* 2016;12(4):460–7.
- [18] Aly F, Miller AA, Jameson MG, Metcalfe PE. A prospective study of weekly intensity modulated radiation therapy plan adaptation for head and neck cancer: Improved target coverage and organ at risk sparing. *Australasian Physical and Engineering Sciences in Medicine* 2019;42(1):43–51.
- [19] Figen M, Öksüz DÇ, Duman E, Prestwich R, Dyker K, Cardale K, Ramasamy S, Murray P, Şen M. Radiotherapy for head and neck cancer: Evaluation of triggered adaptive replanning in routine practice. *Frontiers in Oncology* 2020;59(4):960-70.
- [20] Bobić M, Lalonde A, Sharp GC, Grassberger C, Verburg JM, Winey BA, Lomax AJ, Paganetti H. Comparison of weekly and daily online adaptation for head and neck intensity-modulated proton therapy. *Physics in Medicine and Biology* 2021;66(5):10.1088/1361-6560/abe050.
- [21] Gupta A, Dunlop A, Mitchell A, McQuaid D, Nill S, Barnes H, Newbold K, Nutting C, Bhide S, Oelfke U, Harrington KJ, Wong KH. Online adaptive radiotherapy for head and neck cancers on the MR linear accelerator: Introducing a novel modified adapt-to-shape approach. *Clinical and Translational Radiation Oncology* 2021; 32:48–51.
- [22] Beetz I. NTCP models for patient-rated xerostomia and sticky saliva after treatment with intensity modulated radiotherapy for head and neck cancer: The role of dosimetric and clinical factors. *Radiotherapy and Oncology* 2012;105(1):101–6.
- [23] Wopken K. Development of a multivariable normal tissue complication probability (NTCP) model for tube feeding dependence after curative radiotherapy/chemo- radiotherapy in head and neck cancer. *Radiotherapy and Oncology* 2014;113(1):95–101.
- [24] Dijkema T, Raaijmakers CP, Ten Haken RK, Roesink JM, Braam PM, Houweling AC, Moerland MA, Eisbruch A, Terhaard CH. Parotid gland function after radiotherapy: The combined Michigan and Utrecht experience. *International Journal of Radiation Oncology, Biology, Physics* 2010;78(2):449–53.
- [25] Lyman JT. Complication probability as assessed from dose-volume histograms. *Radiation Research. Supplement* 1985;8:S13–9.
- [26] Kutcher GJ, Burman C. Calculation of complication probability factors for non- uniform normal tissue irradiation: The effective volume method. *International Journal of Radiation Oncology, Biology, Physics* 1989;16(6):1623–30.
- [27] Christianen MEMC. Predictive modelling for swallowing dysfunction after primary (chemo) radiation: Results of a prospective observational study. *Radiotherapy and Oncology: Journal of the European Society for Therapeutic Radiology and Oncology* 2012;105(1):107–14.